atoms

MDPI

Article

Current Status and Developments of the Atomic Database on Rare-Earths at Mons University (DREAM)

Pascal Quinet [1,2,*] and Patrick Palmeri [1]

[1] Physique Atomique et Astrophysique, Université de Mons, B-7000 Mons, Belgium; patrick.palmeri@umons.ac.be
[2] IPNAS, Université de Liège, B-4000 Liège, Belgium
* Correspondence: Pascal.Quinet@umons.ac.be; Tel.: +32-65-373629

Received: 21 February 2020; Accepted: 31 March 2020; Published: 2 May 2020

Abstract: The main purpose of the Database on Rare Earths At Mons University (DREAM) is to provide the scientific community with updated spectroscopic parameters related to lanthanide atoms (Z = 57–71) in their lowest ionization stages. The radiative parameters (oscillator strengths and transitions probabilities) listed in the database have been obtained over the past 20 years by the Atomic Physics and Astrophysics group of Mons University, Belgium, thanks to a systematic and extensive use of the pseudo-relativistic Hartree-Fock (HFR) method modified for taking core-polarization and core-penetration effects into account. Most of these theoretical results have been validated by the good agreement obtained when comparing computed radiative lifetimes and accurate experimental values measured by the time-resolved laser-induced fluorescence technique. In the present paper, we report on the current status and developments of the database that gathers radiative parameters for more than 72,000 spectral lines in neutral, singly-, doubly-, and triply-ionized lanthanides.

Keywords: atomic database; lanthanides; oscillator strengths; transition probabilities

1. Introduction

The atomic structures and radiative properties characterizing the lowest ionization stages of lanthanide elements, from La (Z = 57) to Lu (Z = 71), have been the subject of many experimental and theoretical investigations during the last years. At our last consultation (January 2020), the NIST atomic spectra bibliographic database [1] counted 1816 references on energy levels and 480 references on radiative transition rates related to the first four spectra (I–IV) of lanthanide atoms. The cumulative numbers of relevant papers published over the last decades are reported in Figures 1 and 2, respectively. These figures are the result of a steady increase of publications since the 1950s, demonstrating the growing interest for the atomic data characterizing such heavy atomic species. This is mainly due to the fact that the remarkably rich spectra arising from lanthanide ions provide an essential source of information for the development of other fields, mainly in astrophysics and the lighting industry (see, e.g., [2–6]).

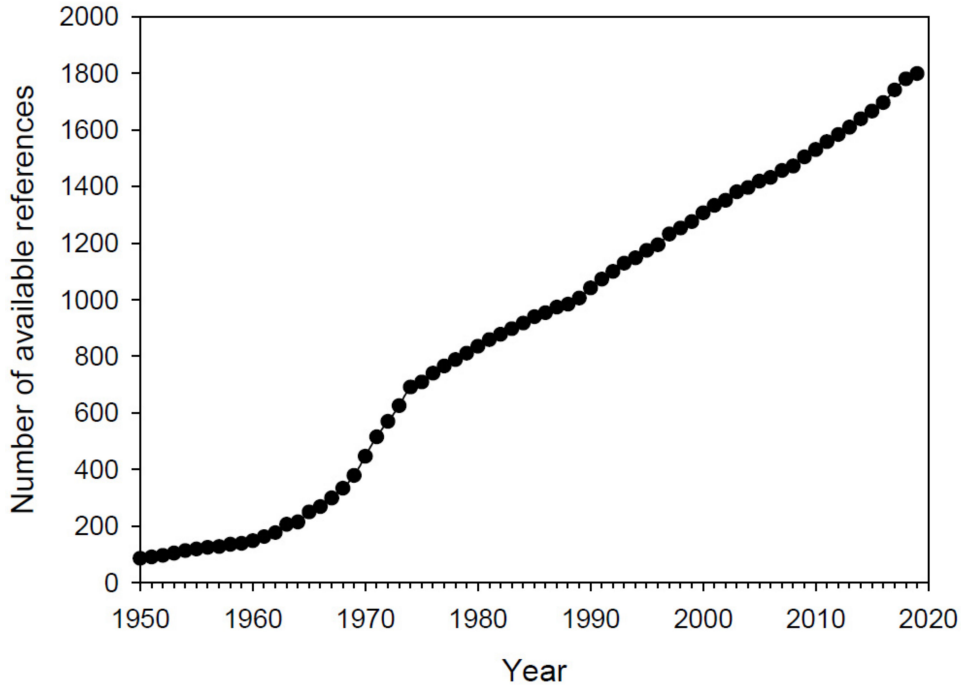

Figure 1. Cumulative number of available references related to atomic energy levels for neutral, singly-, doubly- and triply-ionized lanthanides taken from the NIST bibliographic database [1].

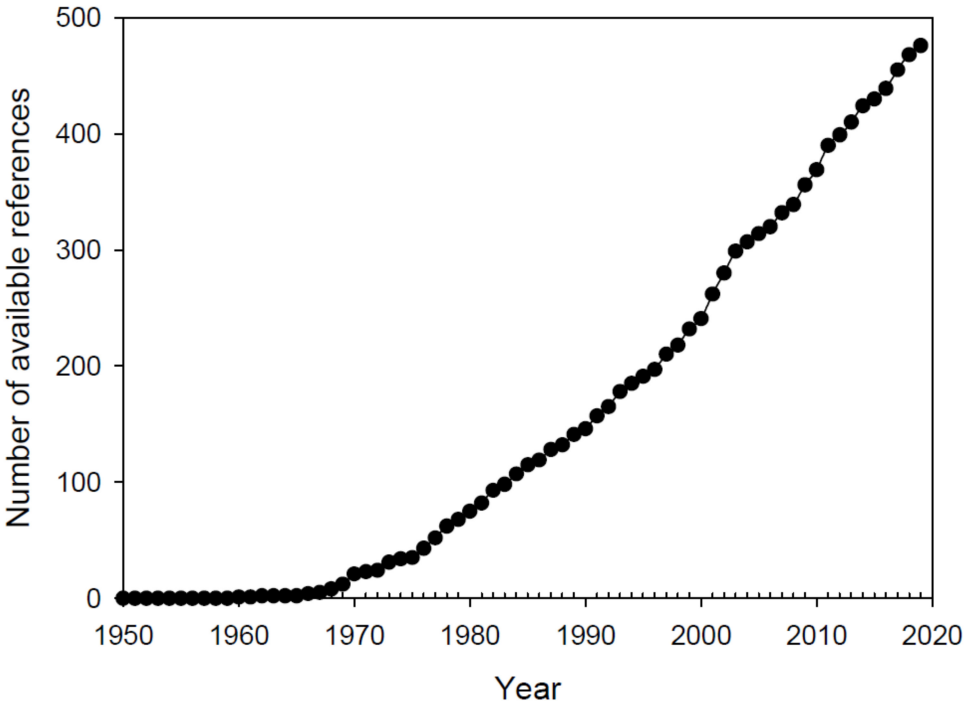

Figure 2. Cumulative number of available references related to radiative parameters (oscillator strengths and transition probabilities) for neutral, singly-, doubly- and triply-ionized lanthanides taken from the NIST bibliographic database [1].

In astrophysics, many lines of neutral, singly-and doubly-ionized lanthanides have been identified in the high-resolution spectra of chemically peculiar stars. The most striking example is probably the roAp star HD 101065, better known as the Przybylski's star, in which the observation of hundreds of lanthanide lines allowed to deduce abundances in these elements of several orders of magnitude greater than the solar values (see, e.g., [7–9]). The lanthanides are particularly important because

they form a group of contiguous elements in which patterns of abundance may be observed and investigated in connection with stellar nucleosynthesis and chemical fractionation [10].

Another important astrophysical application of lanthanide elements concerns the new hot topic of neutron star mergers. Indeed, the ejecta from neutron star mergers produce an electromagnetic signal that can be used, together with the detection of gravitational waves, to locate the source and to study the physics of these mergers. The r-process nucleosynthesis in these ejecta may lead to radioactively powered transients called kilonovae. The timescale and peak luminosity of these transients depend on the composition of the ejecta, which determines the local heating rate from nuclear decays and the opacity which can drastically be increased by lanthanides, as mentioned in [11–13]. The largest remaining uncertainty in kilonova emission relates to missing information about the wavelength dependent opacity of the ejecta, mostly because of the lack of relevant atomic data for the lowest ionization stages of lanthanides [14,15].

Because of their unusual luminescent properties, triply ionized lanthanide atoms also play an important role in photonics, laser physics, biotechnology, medical diagnostics, and lighting industry, see, e.g., [16–19]. All of these ions, except La IV, are characterized by a ground electronic configuration of the type [Xe]$4f^k$with k varying from 1 (Ce IV) to 14 (Lu IV) which is largely responsible for their interesting photophysical properties such as long-lived luminescence and sharp absorption and emission lines. Reliable information about the atomic structures and radiative parameters of triply charged lanthanide ions is therefore essential for analyzing and understanding their light emission.

For all these reasons, about 20 years ago, we started systematic and detailed investigations of + four spectra of lanthanide elements. In the present paper, we briefly remind how these radiative parameters were determined, we present an overview of the current status and developments of DREAM, and we give some remarkable examples of use of the data available in this database.

2. Atomic Structure and Radiative Rate Calculations

The lowest ionization stages of lanthanide atoms are generally characterized by strongly interacting low lying configurations of the type $4f^k$, $4f^{k-1}nl$, $4f^{k-2}nln'l'$ and $4f^{k-3}nln'l'n''l''$. Moreover, the well-known collapse of the 4f orbital occurring at lanthanum is enhanced when the number of 4f electrons increases which makes the atomic structure calculations very difficult, as described in [6]. In all the lanthanide species considered in our theoretical investigations, the same computational approach was used, namely the one based on the pseudo-relativistic Hartree-Fock (HFR) method originally introduced by Cowan [20], and modified for taking core-polarization effects into account, giving rise to the so-called HFR+CPOL approach. In this latter, described in detail in many of our previous papers (see, e.g., [21–23]), the largest part of the intravalence correlation is represented within a configuration interaction scheme, i.e., by explicitly including a set of electronic configurations in the physical model, while core-valence correlation is approximated by a core-polarization (CPOL) model potential depending on two parameters, namely the dipole polarizability, α_d, of the ionic core, for which numerical values can be found in the literature (see, e.g., [24,25]), and the cut-off radius, r_c, that is arbitrarily chosen as a measure of the size of the ionic core. In practice, this latter parameter is usually chosen to be equal to the HFR mean value $<r>$ for the outermost ionic core orbital. In order to allow for a more accurate treatment of core-valence interactions, we added a further correction to account for the penetration of the core by the valence electrons, according to the formalism developed by Hameed and coworkers [26,27].

In addition, for each atomic system, the radial parameters corresponding to the configuration average energies (E_{av}), the monoconfiguration (F^k, G^k) and configuration interaction (R^k) Slater integrals, the spin-orbit parameters (ζ_{nl}) and, if needed, the effective interaction parameters (α, β, γ) [20] were adjusted in a semi-empirical least-squares fit to reduce as much as possible the differences between the calculated energy levels and the available experimental values. This approach, although strongly dependent upon the quantity and the quality of the observed energy levels, allowed us to optimize the eigenvalues and eigenstates, and thus the computed wavelengths, radiative lifetimes,

transition probabilities and oscillator strengths for most of the lanthanide elements considered in our work. However, in some cases, the number of available experimental energy levels was found to be too limited to perform a satisfactory fit. This can be illustrated by considering the two specific examples of Pr I [28] and Pr II [29]. In Pr I, according to the NIST compilation [1], among the 8421 possible levels belonging to the lowest odd- and even-parity configurations, namely $4f^36s^2$, $4f^35d6s$, $4f^25d6s6p$, $4f^26s^26p$, $4f^25d^26p$, $4f^25d6s^2$, $4f^25d^26s$, $4f^36s6p$ and $4f^35d6p$, only 410 have been determined experimentally, with unambiguous labelling. In Pr II, for the low-lying even-parity configurations $4f^4$, $4f^36p$, $4f^25d^2$, $4f^25d6s$ and $4f^26s^2$, only 55 levels are listed in the NIST compilation on a total of 1033 possible levels. In such cases, the scarcity of experimentally established energy levels obviously makes it completely unthinkable a reliable least-squares fitting procedure of the calculated eigenvalues of the Hamiltonian, thus highlighting the need for new basic spectral analyses in the laboratory, especially for neutral and singly ionized lanthanide atoms.

The results we have obtained so far concerning the theoretical determination of radiative data for lanthanide atoms, in their first four ionization stages, are listed in Table 1, together with the corresponding references in which the details of computations can be found.

3. Comparisons with Experimental Data

In view of their complexity, modelling the atomic structures and computing the radiative parameters in neutral and lowly ionized lanthanides represent a difficult task so that it is necessary to assess the quality of the results obtained through comparisons with laboratory measurements. In order to estimate the reliability of the theoretical models considered in our work, a large number of experimental investigations were also carried out over the past 20 years. More precisely, for many lanthanide ions, atomic lifetime measurements were carried out using time-resolved laser-induced-fluorescence (TR-LIF) spectroscopy, mainly with the instrumental setup developed at the Lund Laser Centre, Sweden. It is well known that this technique has many advantages including the elimination of cascade problems through different types of selective excitation, such as one-step, two-step or two-photon excitation, and the use of various laser dyes. The accessible lifetimes range generally from 1 ns to several hundreds of ns, with uncertainties of a few percent in the large majority of cases. This technique, described in many papers, see, e.g., [30,31], is based of the production of free atoms and ions within a plasma created by laser ablation in which a laser pulse of a few ns duration irradiates a metallic foil placed in a vacuum chamber. The expanding laser-produced plasma is then crossed by another laser whose wavelength allows to selectively populate the considered level. The fluorescence generated is collected by a fused-silica lens, and then appropriately filtered by a monochromator, to be finally detected by a microchannel-plate photomultiplier tube. The decay curves are analyzed and the lifetimes are extracted by a least-squares fit of a single exponential decay, convoluted to the data by the measured laser pulse, if necessary, i.e., in the case of lifetime values similar to the laser pulse duration.

In our common work with the Lund Laser Centre, we managed to measure the radiative lifetimes for a total of 324 energy levels belonging to La I, La III, Ce II, Ce IV, Pr I, Pr II, Pr III, Nd I, Nd II, Nd III, Sm II, Sm III, Eu III, Tb III, Dy III, Ho III, Er II, Er III, Tm III, Yb II, Yb III, Lu I, Lu II, and Lu III lanthanide ions. These experimental measurements, for which the corresponding references are quoted in Table 1, were systematically compared with the lifetime values deduced from our calculations. In most cases, an agreement within a few percent was found except for a limited number of cases that could generally be explained by large mixings occuring in the level compositions, by the fragmentary knowledge of the energy level schemes for some ions or by dubious level assignments in the published experimental level values. In fact, for the whole set of lanthanide ions considered in our work, we found a mean ratio between the calculated and the experimental lifetimes, τ (CALC)/τ (EXP), equal to 0.98 ± 0.23, where the uncertainty corresponds to the standard deviation of the mean. All the details of these comparisons can be found in the papers referred to in the DREAM database and in Table 1, while a general overview is shown in Figure 3 where the ratio τ (CALC)/τ (EXP) is plotted against τ

(CALC) for all the levels of lanthanide elements for which the radiative lifetimes were experimentally determined in our work.

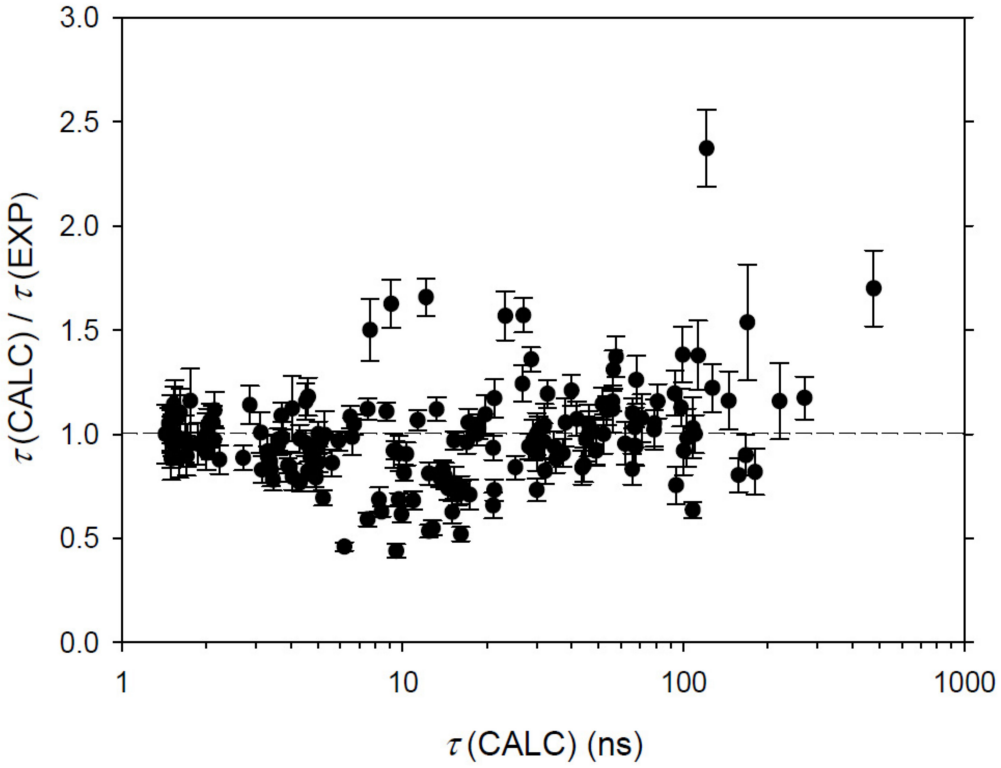

Figure 3. Comparison between the calculated and experimental radiative lifetimes (τ) obtained for all the lanthanide ions considered in our previous works. The calculations were performed using the HFR+CPOL method while the measurements were carried out by TR-LIF spectroscopy. The dashed line indicates unity.

Note that atomic lifetime measurements were also performed for several lanthanide ions using the same TR-LIF experimental technique in other laboratories, mainly at Jilin University (Changshun, China) and Wisconsin University (Madison, USA). In some instances, these measurements were compared with our calculations, giving also rise to a good overall agreement. An example of such an agreement is shown in Figure 2 of our recent paper dedicated to neutral lanthanum [32], this figure illustrating the comparison between our computed HFR+CPOL radiative lifetimes and the TR-LIF experimental values measured at Madison [33]. In this case, the mean ratio τ (CALC)/τ (EXP) was found to be equal to 0.94 ± 0.22 for 70 La I energy levels from 15,000 to 32,140 cm^{-1}.

In addition, experimental transition probabilities and oscillator strengths were published, mainly by the Jilin and Wisconsin groups, for some lowly charged lanthanide ions. These results were generally obtained by combining accurate TR-LIF radiative lifetimes with branching fraction measurements performed in emission spectra collected using grating or Fourier transform spectrometers. In Table 2, we give a comparison between the oscillator strengths extracted from the DREAM database and the available experimental results for four specific lanthanide ions, i.e. Sm III [34], Eu III [35], Tm III [36], and Yb III [37]. As it can be seen, the agreement between both sets of gf-values is very good, the average deviation being found to be within 34% when considering the 135 transitions of Table 2 with calculated log gf-values larger than -2, this deviation being even reduced to 14% when considering only the 78 strongest lines with log gf-values greater than -1. An overview of this comparison is illustrated in Figure 4. This is further confirmation that the DREAM data are trustworthy, especially for the most intense transitions.

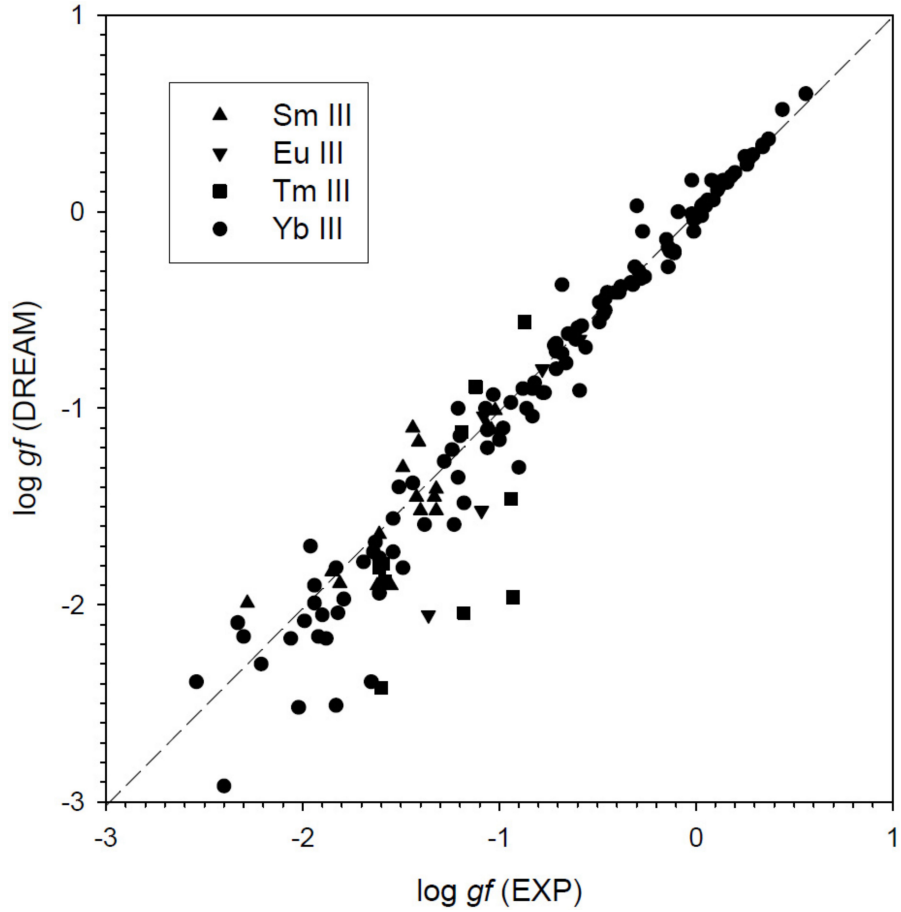

Figure 4. Comparison between the calculated oscillator strengths tabulated in the DREAM database and the experimental values obtained for Sm III [34], Eu III [35], Tm III [36], and Yb III [37].

4. Current Status and Developments of the DREAM Database

The DREAM database contains information concerning the wavelengths, the oscillator strengths and the transition probabilities for spectral lines of neutral, singly-, doubly- and triply ionized lanthanides. The different available spectra are classified in order of increasing Z-values, and for a given Z, according to the ionization degree. For each line in a specific spectrum, the tables show, respectively:

- The wavelength (in Å) deduced from the experimental energy levels. These wavelengths are given in air above 2000 Å and in vacuum below that limit.
- The lower level of the transition represented by its experimental value (in cm^{-1}), its parity ((e) for even and (o) for odd) and its J-value. Level energies (rounded values), are taken from the NIST compilations [1] and from subsequent publications.
- The upper level of the transition presented in the same way as for the lower level.
- The calculated oscillator strength, log gf, where $g = 2J + 1$ is the statistical weight of the lower level of the transition. In general, only transitions for which log $gf > -4.0$ are reported in the tables.
- The calculated transition probability, gA in s^{-1}, where $g = 2J + 1$ is the statistical weight of the upper level of the transition.
- The cancellation factor, CF, as defined by Cowan [20]. Small values of this factor (typically $CF < 0.05$) indicate transitions affected by severe cancellation effects and should therefore be taken with some care.

The details about the computational procedures are given in the different publications corresponding to the atomic systems considered and appearing at the top of each table. For some ions,

experimental oscillator strengths and transition probabilities or normalized log *gf*- and *gA*-values using measured lifetimes are given. In these cases, EXPT or NORM appears in the last column of the tables.

At present, more than 72,000 spectral lines are listed in the DREAM database. They concern La I, La III, Ce II, Ce III, Pr II, Pr III, Pr IV, Nd II, Nd III, Nd IV, Sm II, Sm III, Eu III, Gd III, Tb III, Dy III, Ho III, Er II, Er III, Tm II, Tm III, Tm IV, Yb II, Yb III, Yb IV, Lu I, Lu II, and Lu III. This represents about 75 times more lines with transition probabilities than those currently available for the same ions in the NIST database [1]. For each of these ions, the exact number of lines reported in the DREAM database is given in Table 3 while a sample of data, corresponding to Lu II, is shown in Table 4.

It is also interesting to mention that a rather small number of computed transition rates reported in the DREAM database were found to be affected by strong cancellation effects (with $CF < 0.05$), indicating that the associated oscillator strengths could be unreliable [20]. Moreover we note that a large majority of these 'uncertain' transitions correspond to the weaker ones, with log *gf*-values generally smaller than -2. This is illustrated in Figure 5 where the *CF*-factors are plotted as a function of log *gf* for all Ce II and Pr III lines listed in the DREAM database.

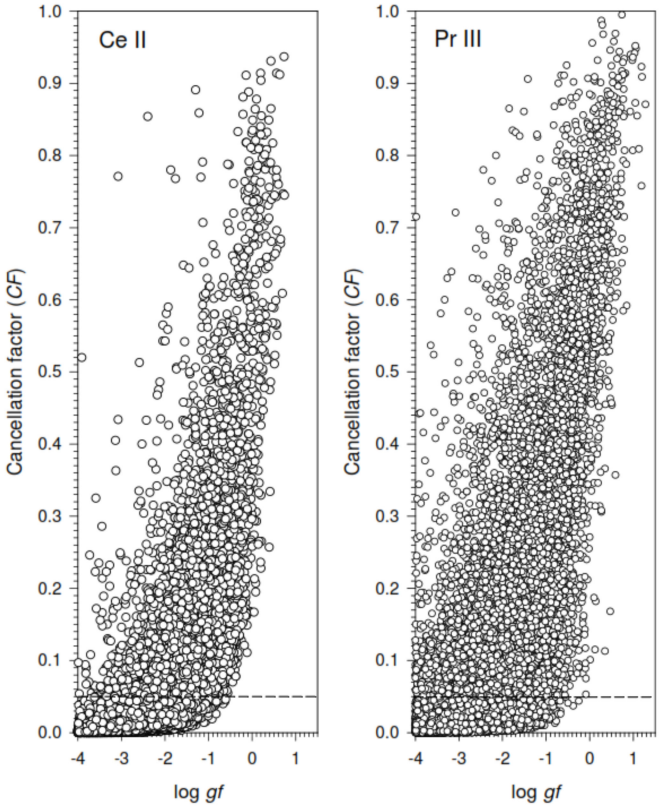

Figure 5. Cancellation factors (*CF*) plotted as a function of log *gf*-values as reported in the DREAM database for Ce II and Pr III spectral lines. The dashed lines correspond to $CF = 0.05$.

A complete list of all the papers we have published regarding our theoretical and experimental investigations of lanthanide elements is also given in the database.

5. Some Examples of Uses of Atomic Data from DREAM

Since the creation of DREAM in 1999 [23], the database has been quoted several dozens times in the literature and the data compiled therein have been extensively used in different astrophysical studies. For instance, the important impact of this database on various astrophysical issues was already discussed by Jorissen [38] while its key role in the great improvement of the abundance patterns of neutron capture elements for metal poor stars was highlighted by Ryabchikova & Mashonkina [39] and Monier [40]. As stated in [39], the atmospheric modelling of the famous Przybylski's star (HD 101065),

whose spectrum consists totally of lanthanide lines with a small number of other lines, became possible thanks to the use of oscillator strengths taken from the DREAM database. Let us also mention that, to ensure greater visibility, most of the DREAM data were incorporated into larger databases such as the Vienna Atomic Line Database (VALD) [41] and the Virtual Atomic and Molecular Data Center (VAMDC) [42].

Another remarkable usefulness of this database concerns the line at 6708.1 Å which was previously identified in some heavily s-process enriched post-AGB stars as being due to lithium, despite the redward shift of about 0.2 Å compared to other photospheric lines. This shift was then explained by hypothetical line formation in infalling circumstellar gas or photospheric downdrafts. Using the available atomic data from DREAM, this line could be safely identified as not being due to Li but coming from a Ce II transition at 6708.099 Å, the cerium abundance derived from this single line being comparable to the one deduced from other Ce II lines in the spectra [43]. Moreover, no inclusion of a significant amount of lithium at photospheric wavelength was needed in the synthesis of three highly s-process enriched stars, namely IRAS 05341+0852, IRAS 06530-0213, and IRAS 05113+1347, allowing to conclude that there was no evidence for in situ Li production and thus no need to invoke special non-standard mixing during the AGB evolution to explain the supposed high abundance of this fragile element in these stars. Using the DREAM database, a succesful systematic search for lines of elements beyond the baryum-peak could also be carried out in spectra of various s-process enriched post-AGB stars, leading, for the first time, to the determination of high abundances of elements heavier than europium, such as Gd, Yb and Lu, in these objects [44].

The use of oscillator strengths compiled in the DREAM database also allowed to identify new lanthanide lines in many different high-resolution astrophysical spectra and to deduce reliable abundances of rare earth elements (sometimes up to several orders of magnitude higher than the solar values in the case of various chemically peculiar stars), see, e.g., [45–56]. To give just one noteworthy specific example, we will mention the recent multicolour photometric investigation of the eclipsing binary system HD 66051 [53] carried out using, among other data, the spectroscopic parameters of the second and third spectra of lanthanides taken from the DREAM database. Thanks to a detailed analysis of the abundance patterns, the authors came to the conclusion that the primary component of this uncommon system is a slowly rotating late B-type star with a highly peculiar composition reminiscent of the singular HgMn related star HD 65949, where most of the heavy elements, in particular the lanthanides, are overabundant, while the secondary component is estimated to be a slowly rotating A-type star. As stated in [53], the unique configuration of HD 66051 opens up intriguing possibilities for future research, which might eventually and significantly contribute to the understanding of such diverse phenomena as atmospheric structure, mass transfer, magnetic fields, photometric variability and the origin of chemical anomalies observed in HgMn stars and related objects.

Finally, let us also mention the use of the atomic data compiled in the DREAM database in the context of neutron star mergers, as for example in two recent works published by Tanaka et al. [57,58]. In the first one, the authors performed radiative transfer simulations for neutron star merger ejecta powered by radioactive energy of r-process nuclei including, for the first time, all the r-process elements from gallium to U, thus including in particular the data for lanthanide elements available in the DREAM database. They could show that the opacity of the neutron star ejecta was higher than previously expected by a factor of about 100 due to many transitions of r-process elements. In the second study, three-dimensional, time-dependent, multi-frequency Monte Carlo radiative transfer simulations were performed for radioactively powered emission from black hole—neutron star mergers by taking into account the wavelength-dependent opacities of r-process elements using relevant atomic data among which those available in the DREAM database. This study allowed the authors to deduce a noteworthy property whereby, when the tidally disrupted black hole—neutron star merger ejecta are confined to a small solid angle, the emission tends to be bluer than that from neutron star—neutron star merger ejecta for a given total luminosity, which makes it possible to distinguish black hole—neutron star merger events from neutron star—neutron star merger events by multi-band observations of the radioactively

powered emission. Such observations can also provide information on the progenitors of gravitational wave sources and the nature of compact objects merging.

6. Conclusions

The DREAM database currently contains radiative parameters (wavelengths, oscillator strengths, transition probabilities) for about 72,700 spectral lines belonging to 28 different lanthanide atoms and ions. The large majority of the transition rates were obtained using the relativistic Hartree-Fock method including core-polarization and core-penetration effects and were validated by the good agreement obtained when comparing computed radiative lifetimes and accurate experimental values measured by the time-resolved laser-induced fluorescence technique. The reliability of the results reported in the database was also confirmed by the good agreement observed between the tabulated data and the most accurate experimental radiative lifetimes and/or transition probabilities recently published for some lanthanide ions. The DREAM database is certainly the most comprehensive at present available for spectroscopic parameters related to the lowest ionization stages of lanthanide elements and it is expected that it will be updated in the light of the new atomic structure calculations we intend to perform in the future for these species of great interest in many different scientific fields. However, new detailed semi-empirical calculations are largely compromised by the obvious lack of fundamental experimental data, in particular with regard to energy levels belonging to neutral and singly ionized lanthanides for which basic spectroscopic term analyses are urgently requested. Accurate branching fraction measurements, obtained using Fourier transform spectroscopy for example, would also be of great interest in order to provide, when combined with the available radiative lifetimes, new experimental transition probabilities in the many ions where such data have not yet been published. This would allow to further refine the estimation of uncertainties related to the calculated radiative parameters tabulated in the DREAM database.

Table 1. Experimental and theoretical methods used in our work for the determination of radiative parameters in lanthanide elements (Z = 57–71) and related references.

Z	Ion	TR + LIF Measurements	HFR + CPOL Calculations	References
57	La I		X	[32]
		X	X	[59]
	La III	X	X	[60]
	La IV		X	[61]
58	Ce II		X	[62]
		X	X	[63]
	Ce III		X	[64]
	Ce IV	X	X	[65]
59	Pr I	X	X	[28]
	Pr II	X	X	[29]
	Pr III		X	[66]
		X	X	[67]
	Pr IV		X	[68]
60	Nd I	X	X	[28]
	Nd II	X	X	[69]
	Nd III	X	X	[70]
	Nd IV		X	[71]
61	Pm II		X	[72]
			X	[73]
62	Sm II	X	X	[74]
	Sm III	X	X	[34]
63	Eu III	X	X	[75]
64	Gd III		X	[76]
65	Tb III	X	X	[77]
66	Dy III	X	X	[78]

Table 1. *Cont.*

Z	Ion	TR + LIF Measurements	HFR + CPOL Calculations	References
67	Ho III	X	X	[79]
		X	X	[80]
68	Er II	X	X	[81]
	Er III	X	X	[82]
69	Tm II		X	[83]
	Tm III	X	X	[84]
	Tm IV		X	[85]
70	Yb II		X	[86]
		X	X	[87]
		X	X	[88]
	Yb III	X	X	[89]
		X	X	[90]
	Yb IV		X	[91]
71	Lu I	X	X	[92]
		X	X	[93]
	Lu II	X	X	[21]
		X	X	[92]
	Lu III	X	X	[60]
		X	X	[92]

Table 2. Comparison between the oscillator strengths taken from DREAM and available experimental data for Sm III, Eu III, Tm III and Yb III.

Wavelength [a]	Lower Level [b]			Upper Level [b]			Log *gf*	
	E (cm^{-1})	*P*	*J*	*E* (cm^{-1})	*P*	*J*	DREAM	EXP
				Sm III				
2709.054	814	(e)	2	37,716	(o)	3	−1.90	−1.62 [c]
2728.568	293	(e)	1	36,932	(o)	2	−1.83	−1.85 [c]
2759.842	1493	(e)	3	37,716	(o)	3	−1.41	−1.32 [c]
2767.859	814	(e)	2	36,932	(o)	2	−1.45	−1.42 [c]
2820.901	1493	(e)	3	36,932	(o)	2	−1.64	−1.61 [c]
2820.995	2298	(e)	4	37,716	(o)	3	−1.52	−1.40 [c]
2829.347	1493	(e)	3	36,826	(o)	4	−1.10	−1.44 [c]
2846.994	814	(e)	2	35,928	(o)	3	−1.17	−1.41 [c]
2854.572	293	(e)	1	35,315	(o)	2	−1.30	−1.49 [c]
2893.652	2278	(e)	4	36,826	(o)	4	−1.09	−1.06 [c]
2897.611	814	(e)	2	35,315	(o)	2	−1.89	−1.81 [c]
2903.143	1493	(e)	3	35,928	(o)	3	−1.45	−1.33 [c]
2955.793	1493	(e)	3	35,315	(o)	2	−1.11	−1.04 [c]
2966.969	3132	(e)	5	36,826	(o)	4	−1.01	−1.02 [c]
2970.889	2278	(e)	4	35,928	(o)	3	−1.01	−1.06 [c]
3392.261	293	(e)	1	29,764	(o)	2	−1.99	−2.28 [c]
3453.209	814	(e)	2	29,764	(o)	2	−1.52	−1.32 [c]
3536.165	1493	(e)	3	29,764	(o)	2	−1.90	−1.55 [c]
				Eu III				
2375.461	0	(o)	3.5	42,084	(e)	4.5	−0.65	−0.59 [d]
2444.387	0	(o)	3.5	40,898	(e)	2.5	−1.52	−1.09 [d]
2446.005	0	(o)	3.5	40,871	(e)	3.5	−0.80	−0.78 [d]
2513.761	0	(o)	3.5	39,769	(e)	2.5	−1.04	−1.08 [d]
2522.144	0	(o)	3.5	39,637	(e)	2.5	−2.05	−1.36 [d]

Table 2. *Cont.*

Wavelength [a]	Lower Level [b]			Upper Level [b]			Log *gf*	
	E (cm^{-1})	P	J	E (cm^{-1})	P	J	DREAM	EXP
				Tm III				
2099.107	0	(o)	3.5	47,624	(e)	2.5	−0.89	−1.12 [e]
2123.800	0	(o)	3.5	47,071	(e)	4.5	−1.88	−1.58 [e]
2136.675	0	(o)	3.5	46,787	(e)	3.5	−1.79	−1.59 [e]
2182.979	0	(o)	3.5	45,795	(e)	3.5	−1.12	−1.19 [e]
2185.939	0	(o)	3.5	45,733	(e)	3.5	−0.56	−0.87 [e]
2573.221	8774	(o)	2.5	47,624	(e)	2.5	−2.42	−1.60 [e]
2700.398	8774	(o)	2.5	45,795	(e)	3.5	−1.81	−1.61 [e]
2704.928	8774	(o)	2.5	45,733	(e)	3.5	−2.04	−1.18 [e]
3273.913	0	(o)	3.5	30,536	(e)	4.5	−1.46	−0.94 [e]
3629.092	0	(o)	3.5	27,547	(e)	3.5	−1.96	−0.93 [e]
5325.252	8774	(o)	2.5	27,547	(e)	3.5	−2.97	−1.60 [e]
				Yb III				
2029.544	39,721	(o)	1	88,977	(e)	2	−1.59	−1.38 [f]
2078.056	72,140	(e)	3	120,247	(o)	4	0.16	0.08 [f]
2086.288	34,991	(o)	3	82,907	(e)	2	−2.30	−2.21 [f]
2086.534	82,546	(e)	3	130,457	(o)	2	0.03	0.03 [f]
2087.375	39,721	(o)	1	87,613	(e)	1	−1.73	−1.64 [f]
2087.985	72,487	(e)	4	120,365	(o)	3	0.16	−0.02 [f]
2093.135	72,487	(e)	4	120,247	(o)	4	−0.10	−0.27 [f]
2098.249	82,907	(e)	2	130,551	(o)	3	0.03	−0.30 [f]
2102.132	34,991	(o)	3	82,546	(e)	3	−2.05	−1.90 [f]
2155.505	43,019	(o)	3	89,397	(e)	3	−1.16	−1.00 [f]
2169.796	42,425	(o)	4	88,498	(e)	4	−2.16	−2.30 [f]
2175.221	43,019	(o)	3	88,977	(e)	2	−3.13	−2.51 [f]
2198.143	43,019	(o)	3	88,498	(e)	4	−1.48	−1.18 [f]
2202.272	33,386	(o)	2	78,779	(e)	3	−0.90	−0.88 [f]
2227.712	43,623	(o)	5	88,498	(e)	4	−1.76	−1.61 [f]
2231.567	33,386	(o)	2	78,183	(e)	2	−2.16	−1.92 [f]
2240.112	34,656	(o)	4	79,283	(e)	4	0.34	0.34 [f]
2244.284	44,854	(o)	2	89,397	(e)	3	−0.03	0.00 [f]
2257.033	34,991	(o)	3	79,283	(e)	4	0.06	0.06 [f]
2262.267	45,208	(o)	3	89,397	(e)	3	0.18	0.18 [f]
2265.665	44,854	(o)	2	88,977	(e)	2	0.20	0.20 [f]
2265.683	34,656	(o)	4	78,779	(e)	3	−0.46	−0.49 [f]
2282.993	34,991	(o)	3	78,779	(e)	3	0.33	0.34 [f]
2283.994	45,208	(o)	3	88,977	(e)	2	−0.62	−0.65 [f]
2284.161	39,141	(o)	3	82,907	(e)	2	−3.21	−2.52 [f]
2303.165	39,141	(o)	3	82,546	(e)	3	−3.98	−1.97 [f]
2305.334	34,656	(o)	4	78,020	(e)	5	0.60	0.56 [f]
2309.278	45,208	(o)	3	88,498	(e)	4	0.52	0.44 [f]
2314.490	34,991	(o)	3	78,183	(e)	2	0.27	0.27 [f]
2314.820	39,721	(o)	1	82,907	(e)	2	−1.27	−1.28 [f]
2333.288	87,613	(e)	1	130,457	(o)	2	−0.21	−0.11 [f]
2337.971	44,854	(o)	2	87,613	(e)	1	0.04	0.04 [f]
2345.634	40,288	(o)	2	82,907	(e)	2	−2.92	−2.40 [f]
2358.532	40,160	(o)	4	82,546	(e)	3	−2.08	−1.99 [f]
2361.084	47,057	(o)	4	89,397	(e)	3	−0.97	−0.94 [f]
2361.347	45,277	(o)	0	87,613	(e)	1	−0.87	−0.82 [f]
2365.433	37,020	(o)	5	79,283	(e)	4	−0.90	−0.83 [f]
2365.678	40,288	(o)	2	82,546	(e)	3	−3.06	−2.25 [f]

Table 2. *Cont.*

Wavelength [a]	Lower Level [b]			Upper Level [b]			Log *gf*	
	E (cm^{-1})	P	J	E (cm^{-1})	P	J	DREAM	EXP
2367.454	78,020	(e)	5	120,247	(o)	4	0.37	0.37 [f]
2369.991	78,183	(e)	2	120,365	(o)	3	0.03	0.05 [f]
2377.216	88,498	(e)	4	130,551	(o)	3	0.29	0.29 [f]
2403.952	78,779	(e)	3	120,365	(o)	3	0.11	0.11 [f]
2404.618	88,977	(e)	2	130,551	(o)	3	−0.92	−0.78 [f]
2410.046	88,977	(e)	2	130,457	(o)	2	−0.01	0.01 [f]
2410.781	78,779	(e)	3	120,247	(o)	4	−0.77	−0.66 [f]
2412.337	47,057	(o)	4	88,498	(e)	4	−1.14	−1.20 [f]
2429.180	89,397	(e)	3	130,551	(o)	3	0.00	−0.09 [f]
2433.423	79,283	(e)	4	120,365	(o)	3	−0.18	−0.14 [f]
2434.719	89,397	(e)	3	130,457	(o)	2	−0.28	−0.14 [f]
2438.273	37,020	(o)	5	78,020	(e)	5	−1.00	−1.07 [f]
2439.312	48,415	(o)	2	89,397	(e)	3	−0.93	−1.03 [f]
2440.421	79,283	(e)	4	120,247	(o)	4	0.13	0.12 [f]
2464.591	48,415	(o)	2	88,977	(e)	2	−2.39	−1.65 [f]
2490.422	39,141	(o)	3	79,283	(e)	4	−0.68	−0.72 [f]
2491.693	42,425	(o)	4	82,546	(e)	3	−1.70	−1.96 [f]
2506.248	43,019	(o)	3	82,907	(e)	2	−1.81	−1.49 [f]
2522.066	39,141	(o)	3	78,779	(e)	3	−2.52	−2.02 [f]
2529.145	43,019	(o)	3	82,546	(e)	3	−2.17	−1.88 [f]
2550.389	48,415	(o)	2	87,613	(e)	1	−1.73	−1.54 [f]
2555.283	40,160	(o)	4	79,283	(e)	4	−0.67	−0.71 [f]
2560.559	39,141	(o)	3	78,183	(e)	2	−1.94	−1.61 [f]
2566.778	50,029	(o)	1	88,977	(e)	2	−1.10	−0.98 [f]
2567.610	39,085	(o)	6	78,020	(e)	5	0.24	0.26 [f]
2579.563	33,386	(o)	2	72,140	(e)	3	−0.30	−0.29 [f]
2588.607	40,160	(o)	4	78,779	(e)	3	−1.38	−1.44 [f]
2597.219	40,288	(o)	2	78,779	(e)	3	−0.80	−0.71 [f]
2599.148	39,721	(o)	1	78,183	(e)	2	−0.52	−0.47 [f]
2621.107	50,357	(o)	5	88,498	(e)	4	0.16	0.14 [f]
2627.073	44,854	(o)	2	82,907	(e)	2	−0.71	−0.71 [f]
2635.405	51,464	(o)	2	89,397	(e)	3	−1.30	−0.90 [f]
2638.059	40,288	(o)	2	78,183	(e)	2	−0.37	−0.32 [f]
2640.494	40,160	(o)	4	78,020	(e)	5	−1.00	−0.86 [f]
2642.559	34,656	(o)	4	72,487	(e)	4	−0.01	−0.02 [f]
2643.622	51,582	(o)	3	89,397	(e)	3	−0.91	−0.59 [f]
2651.746	45,208	(o)	3	82,907	(e)	2	0.15	0.10 [f]
2652.241	44,854	(o)	2	82,546	(e)	3	0.15	0.16 [f]
2659.973	50,029	(o)	1	87,613	(e)	1	−0.56	−0.49 [f]
2664.935	51,464	(o)	2	88,977	(e)	2	−0.41	−0.41 [f]
2666.136	34,991	(o)	3	72,487	(e)	4	0.28	0.27 [f]
2666.989	34,656	(o)	4	72,140	(e)	3	0.28	0.25 [f]
2673.337	51,582	(o)	3	88,977	(e)	2	−1.00	−1.21 [f]
2677.392	45,208	(o)	3	82,546	(e)	3	−0.14	−0.15 [f]
2691.006	34,991	(o)	3	72,140	(e)	3	−0.59	−0.60 [f]
2708.041	51,582	(o)	3	88,498	(e)	4	−1.56	−1.54 [f]
2712.324	42,425	(o)	4	79,283	(e)	4	−0.36	−0.33 [f]
2749.900	42,425	(o)	4	78,779	(e)	3	−0.20	−0.11 [f]
2755.934	53,123	(o)	3	89,397	(e)	3	−0.38	−0.38 [f]
2756.761	43,019	(o)	3	79,283	(e)	4	−1.20	−1.06 [f]
2765.532	51,464	(o)	2	87,613	(e)	1	−0.69	−0.56 [f]
2788.243	53,123	(o)	3	88,977	(e)	2	−0.33	−0.26 [f]

Table 2. *Cont.*

Wavelength [a]	Lower Level [b]			Upper Level [b]			Log *gf*	
	E (cm^{-1})	*P*	*J*	*E* (cm^{-1})	*P*	*J*	DREAM	EXP
2795.586	43,019	(o)	3	78,779	(e)	3	−0.20	−0.13 [f]
2803.314	53,736	(o)	4	89,397	(e)	3	−0.10	−0.01 [f]
2803.425	43,623	(o)	5	79,283	(e)	4	−0.02	0.03 [f]
2807.223	53,365	(o)	1	88,977	(e)	2	−1.40	−1.51 [f]
2808.527	42,425	(o)	4	78,020	(e)	5	−1.59	−1.23 [f]
2816.912	47,057	(o)	4	82,546	(e)	3	−0.04	−0.01 [f]
2818.715	37,020	(o)	5	72,487	(e)	4	0.06	0.09 [f]
2826.015	53,123	(o)	3	88,498	(e)	4	−1.81	−1.83 [f]
2842.959	43,019	(o)	3	78,183	(e)	2	−0.72	−0.68 [f]
2875.857	53,736	(o)	4	88,498	(e)	4	−0.44	−0.46 [f]
2898.310	48,415	(o)	2	82,907	(e)	2	−0.41	−0.45 [f]
2906.320	43,623	(o)	5	78,020	(e)	5	−0.34	−0.28 [f]
2928.974	48,415	(o)	2	82,546	(e)	3	−1.04	−0.83 [f]
2998.005	39,141	(o)	3	72,487	(e)	4	−0.92	−0.77 [f]
3029.488	39,141	(o)	3	72,140	(e)	3	−0.28	−0.31 [f]
3031.644	45,208	(o)	3	78,183	(e)	2	−1.68	−1.63 [f]
3040.663	50,029	(o)	1	82,907	(e)	2	−1.78	−1.69 [f]
3092.497	40,160	(o)	4	72,487	(e)	4	−0.37	−0.68 [f]
3126.007	40,160	(o)	4	72,140	(e)	3	−0.50	−0.46 [f]
3138.573	40,288	(o)	2	72,140	(e)	3	−1.21	−1.24 [f]
3191.350	51,582	(o)	3	82,907	(e)	2	−0.65	−0.61 [f]
3228.567	51,582	(o)	3	82,546	(e)	3	−0.41	−0.39 [f]
3325.514	42,425	(o)	4	72,487	(e)	4	−1.35	−1.21 [f]
3384.013	53,365	(o)	1	82,907	(e)	2	−0.58	−0.58 [f]
3392.560	43,019	(o)	3	72,487	(e)	4	−2.17	−2.06 [f]
3397.664	53,123	(o)	3	82,546	(e)	3	−2.51	−1.83 [f]
3432.930	43,019	(o)	3	72,140	(e)	3	−2.09	−2.33 [f]
3463.505	43,623	(o)	5	72,487	(e)	4	−2.04	−1.82 [f]
3613.907	50,357	(o)	5	78,020	(e)	5	−1.99	−1.94 [f]
3896.544	53,123	(o)	3	78,779	(e)	3	−1.97	−1.79 [f]
3931.242	47,057	(o)	4	72,487	(e)	4	−1.90	−1.94 [f]
3985.552	47,057	(o)	4	72,140	(e)	3	−2.39	−2.54 [f]
4028.155	53,365	(o)	1	78,183	(e)	2	−1.11	−1.06 [f]

[a] Air wavelengths (in Å) deduced from experimental energy levels. [b] Lower and upper levels of the transitions are represented by their experimental values (in cm^{-1}), their parities ((e) for even and (o) for odd) and their *J*-values. Level energies (rounded values), are taken from the NIST compilation [1] and from subsequent publications. [c] Experimental oscillator strengths, log *gf*, taken from Biémont et al. [34]. [d] Experimental oscillator strengths, log gf, taken from Tian et al. [35]. [e] Experimental oscillator strengths, log gf, taken from Yu et al. [36]. [f] Experimental oscillator strengths, log gf, taken from Öberg and Lundberg [37].

Table 3. Number of lines for which the radiative parameters (wavelengths, oscillator strengths and transition probabilities) are listed in the DREAM database.

Z	Ion	Number of Lines
57	La I	1365
	La III	131
58	Ce II	15,989
	Ce III	2935
59	Pr II	144
	Pr III	18,331
	Pr IV	786
60	Nd II	106
	Nd III	52
	Nd IV	4503

Table 3. *Cont.*

Z	Ion	Number of Lines
62	Sm II	162
	Sm III	81
63	Eu III	893
64	Gd III	44
65	Tb III	913
66	Dy III	1304
67	Ho III	1325
68	Er II	19
	Er III	1308
69	Tm II	7881
	Tm III	1479
	Tm IV	2913
70	Yb II	6792
	Yb III	271
	Yb IV	2770
71	Lu I	44
	Lu II	107
	Lu III	59

Table 4. Sample of data listed in the DREAM database for Lu II lines.

Wavelength [a]	Lower Level [b]			Upper Level [b]			Log *gf* [c]	*gA* [c]	*CF* [d]
1691.406	0	(e)	0	59,122	(o)	1	−0.32	1.11×10^{9}	0.285
1998.034	0	(e)	0	50,049	(o)	1	−1.51	5.10×10^{7}	0.373
2141.245	12,435	(e)	2	59,122	(o)	1	−2.27	7.83×10^{6}	0.009
2195.556	0	(e)	0	45,532	(o)	1	−0.81	2.14×10^{8}	0.603
2392.198	17,333	(e)	2	59,122	(o)	1	−0.02	1.11×10^{9}	0.303
2459.643	12,435	(e)	2	53,079	(o)	3	−2.15	7.86×10^{6}	0.014
2469.265	28,503	(o)	1	68,989	(e)	0	−1.48	3.60×10^{7}	0.315
2536.960	11,796	(e)	1	51,202	(o)	2	−1.26	5.73×10^{7}	0.399
2571.230	14,199	(e)	3	53,079	(o)	3	−0.41	3.94×10^{8}	0.964
2578.785	12,435	(e)	2	51,202	(o)	2	−0.24	5.79×10^{8}	0.519
2613.396	11,796	(e)	1	50,049	(o)	1	−0.19	6.32×10^{8}	0.935
2615.411	0	(e)	0	38,223	(o)	1	0.14	1.36×10^{9}	0.703
2619.259	11,796	(e)	1	49,964	(o)	0	−0.31	4.76×10^{8}	0.923
2657.802	12,435	(e)	2	50,049	(o)	1	−0.12	7.20×10^{8}	0.530
2701.713	14,199	(e)	3	51,202	(o)	2	0.13	1.23×10^{9}	0.583
2738.173	27,264	(o)	0	63,774	(e)	1	−0.66	1.93×10^{8}	0.662
2754.168	12,435	(e)	2	48,733	(o)	3	−0.02	8.37×10^{8}	0.817
2796.633	17,333	(e)	2	53,079	(o)	3	0.09	1.05×10^{9}	0.353
2834.345	28,503	(o)	1	63,774	(e)	1	−0.23	4.93×10^{8}	0.659
2847.505	11,796	(e)	1	46,904	(o)	2	−0.23	4.88×10^{8}	0.807
2894.839	14,199	(e)	3	48,733	(o)	3	0.18	1.21×10^{9}	0.641
2900.303	12,435	(e)	2	46,904	(o)	2	−0.11	6.11×10^{8}	0.403
2911.394	14,199	(e)	3	48,537	(o)	4	0.51	2.51×10^{9}	0.891
2951.683	17,333	(e)	2	51,202	(o)	2	−0.32	3.70×10^{8}	0.823
2963.319	11,796	(e)	1	45,532	(o)	1	−0.24	4.39×10^{8}	0.604
2969.813	11,796	(e)	1	45,459	(o)	2	−0.58	2.00×10^{8}	0.446
3020.541	12,435	(e)	2	45,532	(o)	1	−0.34	3.31×10^{8}	0.828
3027.289	12,435	(e)	2	45,459	(o)	2	−2.64	1.65×10^{6}	0.002
3055.662	17,333	(e)	2	50,049	(o)	1	−2.55	2.03×10^{6}	0.010
3056.720	14,199	(e)	3	46,904	(o)	2	−0.27	3.88×10^{8}	0.853
3077.605	12,435	(e)	2	44,919	(o)	3	0.16	1.01×10^{9}	0.562
3183.731	17,333	(e)	2	48,733	(o)	3	−1.45	2.35×10^{7}	0.045
3191.819	32,453	(o)	2	63,774	(e)	1	−0.04	5.99×10^{8}	0.647
3198.105	14,199	(e)	3	45,459	(o)	2	−0.40	2.63×10^{8}	0.936

Table 4. *Cont.*

Wavelength [a]	Lower Level [b]			Upper Level [b]			Log *gf* [c]	*gA* [c]	*CF* [d]
3249.477	38,223	(o)	1	68,989	(e)	0	−0.25	3.58×10^8	0.710
3254.312	14,199	(e)	3	44,919	(o)	3	−0.17	4.26×10^8	0.926
3364.258	29,407	(e)	2	59,122	(o)	1	−2.84	8.60×10^5	0.010
3380.629	17,333	(e)	2	46,904	(o)	2	−1.80	9.35×10^6	0.041
3397.066	11,796	(e)	1	41,225	(o)	2	−0.11	4.54×10^8	0.649
3472.477	12,435	(e)	2	41,225	(o)	2	−0.22	3.33×10^8	0.932
3507.380	0	(e)	0	28,503	(o)	1	−1.17	3.62×10^7	0.631
3545.118	17,333	(e)	2	45,532	(o)	1	−3.23	3.09×10^5	0.003
3554.416	17,333	(e)	2	45,459	(o)	2	0.19	8.11×10^8	0.798
3623.981	17,333	(e)	2	44,919	(o)	3	−0.81	7.75×10^7	0.515
3699.104	14,199	(e)	3	41,225	(o)	2	−3.97	5.22×10^4	0.001
3782.898	11,796	(e)	1	38,223	(o)	1	−2.90	5.82×10^5	0.015
3876.648	12,435	(e)	2	38,223	(o)	1	−1.09	3.61×10^7	0.214
3912.662	38,223	(o)	1	63,774	(e)	1	−1.50	1.39×10^7	0.746
4184.256	17,333	(e)	2	41,225	(o)	2	−0.44	1.38×10^8	0.469
4223.098	29,407	(e)	2	53,079	(o)	3	−1.79	6.11×10^6	0.250
4259.505	35,652	(e)	0	59,122	(o)	1	−2.99	3.77×10^5	0.008
4262.016	45,532	(o)	1	68,989	(e)	0	−1.36	1.62×10^7	0.394
4342.032	36,098	(e)	2	59,122	(o)	1	−0.60	8.94×10^7	0.278
4430.329	36,557	(e)	1	59,122	(o)	1	−2.78	5.58×10^5	0.096
4433.475	41,225	(o)	2	63,774	(e)	1	−2.66	7.33×10^5	0.875
4505.222	30,889	(e)	3	53,079	(o)	3	−1.66	7.18×10^6	0.940
4586.931	29,407	(e)	2	51,202	(o)	2	−1.72	6.15×10^6	0.347
4785.433	17,333	(e)	2	38,223	(o)	1	−1.91	3.61×10^6	0.008
4839.617	11,796	(e)	1	32,453	(o)	2	−2.18	1.87×10^6	0.473
4843.021	29,407	(e)	2	50,049	(o)	1	−1.56	7.77×10^6	0.443
4858.742	32,504	(e)	4	53,079	(o)	3	−1.41	1.09×10^7	0.073
4865.422	38,575	(e)	2	59,122	(o)	1	−0.59	7.22×10^7	0.401
4921.686	30,889	(e)	3	51,202	(o)	2	−1.20	1.75×10^7	0.812
4994.126	12,435	(e)	2	32,453	(o)	2	−1.14	1.92×10^7	0.401
5172.804	29,407	(e)	2	48,733	(o)	3	−2.72	4.72×10^5	0.045
5278.474	50,049	(o)	1	68,989	(e)	0	−2.00	2.43×10^6	0.232
5458.268	45,459	(o)	2	63,774	(e)	1	−1.74	4.09×10^6	0.906
5476.675	14,199	(e)	3	32,453	(o)	2	−0.42	8.52×10^7	0.432
5480.341	45,532	(o)	1	63,774	(e)	1	−2.97	2.41×10^5	0.511
5602.538	30,889	(e)	3	48,733	(o)	3	−1.82	3.25×10^6	0.068
5664.876	30,889	(e)	3	48,537	(o)	4	−1.40	8.27×10^6	0.974
5713.458	29,407	(e)	2	46,904	(o)	2	−1.52	6.16×10^6	0.118
5887.251	36,098	(e)	2	53,079	(o)	3	−1.48	6.37×10^6	0.047
5926.068	46,904	(o)	2	63,774	(e)	1	−2.38	7.97×10^5	0.700
5983.886	11,796	(e)	1	28,503	(o)	1	−1.15	1.33×10^7	0.507
6159.888	32,504	(e)	4	48,733	(o)	3	0.07	2.05×10^8	0.949
6199.593	29,407	(e)	2	45,532	(o)	1	−0.33	7.99×10^7	0.865
6221.890	12,435	(e)	2	28,503	(o)	1	−0.76	2.99×10^7	0.400
6228.084	29,407	(e)	2	45,459	(o)	2	−1.06	1.52×10^7	0.352
6235.329	32,504	(e)	4	48,537	(o)	4	−0.28	9.01×10^7	0.974
6242.306	30,889	(e)	3	46,904	(o)	2	−0.12	1.30×10^8	0.950
6444.849	29,407	(e)	2	44,919	(o)	3	−1.53	4.74×10^6	0.599
6463.107	11,796	(e)	1	27,264	(o)	0	−1.05	1.43×10^7	0.538
6611.633	17,333	(e)	2	32,453	(o)	2	−2.12	1.15×10^6	0.498
6619.162	36,098	(e)	2	51,202	(o)	2	−0.99	1.57×10^7	0.145
6826.567	36,557	(e)	1	51,202	(o)	2	−1.15	1.02×10^7	0.229
6861.774	30,889	(e)	3	45,459	(o)	2	−2.08	1.19×10^6	0.118
6892.563	38,575	(e)	2	53,079	(o)	3	−1.07	1.20×10^7	0.171
6943.928	35,652	(e)	0	50,049	(o)	1	−1.14	9.98×10^6	0.299
7125.827	30,889	(e)	3	44,919	(o)	3	−0.41	5.04×10^7	0.971
7165.959	36,098	(e)	2	50,049	(o)	1	−1.05	1.14×10^7	0.446
7238.757	49,964	(o)	0	63,774	(e)	1	−1.78	2.12×10^6	0.925
7283.914	50,049	(o)	1	63,774	(e)	1	−1.34	5.73×10^6	0.952
7409.676	36,557	(e)	1	50,049	(o)	1	−1.09	9.78×10^6	0.511

Table 4. *Cont.*

Wavelength [a]	Lower Level [b]			Upper Level [b]			Log *gf* [c]	*gA* [c]	*CF* [d]
7456.998	36,557	(e)	1	49,964	(o)	0	−1.02	1.14×10^7	0.566
7912.340	36,098	(e)	2	48,733	(o)	3	−1.21	6.56×10^6	0.181
7917.535	38,575	(e)	2	51,202	(o)	2	−0.62	2.58×10^7	0.381
7951.592	51,202	(o)	2	63,774	(e)	1	−1.17	7.04×10^6	0.902
8052.519	32,504	(e)	4	44,919	(o)	3	−2.16	7.09×10^5	0.042
8459.158	29,407	(e)	2	41,225	(o)	2	−0.73	1.75×10^7	0.670
8712.766	38,575	(e)	2	50,049	(o)	1	−1.46	3.03×10^6	0.202
8949.629	17,333	(e)	2	28,503	(o)	1	−2.54	2.41×10^5	0.028
9251.408	36,098	(e)	2	46,904	(o)	2	−3.28	4.09×10^4	0.003
9661.679	36,557	(e)	1	46,904	(o)	2	−1.29	3.66×10^6	0.280
9672.391	30,889	(e)	3	41,225	(o)	2	−2.97	7.63×10^4	0.020
9841.516	38,575	(e)	2	48,733	(o)	3	−1.96	7.58×10^5	0.040

[a] Wavelengths (in Å) deduced from experimental energy levels. These wavelengths are given in air above 2000 Å and in vacuum below that limit. [b] Lower and upper levels of the transitions are represented by their experimental values (in cm^{-1}), their parities ((e) for even and (o) for odd) and their *J*-values. Level energies (rounded values), are taken from the NIST compilation [1] and from subsequent publications. [c] Weighted oscillator strengths, log *gf*, and weighted transition probabilities, *gA* in s^{-1}, as computed in our work. [d] Cancellation factors, *CF*, as defined by Cowan [20]. Small values of this factor (typically $CF < 0.05$) indicate transitions affected by severe cancellation effects and should therefore be taken with some care.

Author Contributions: Conceptualization, P.Q. and P.P.; Investigation, P.Q. and P.P.; Methodology, P.Q. and P.P. Both authors were equally involved in the preparation and the writing of the present paper. All authors have read and agreed to the published version of the manuscript.

Funding: This research received no external funding.

Acknowledgments: PQ and PP are respectively Research Director and Research Associate of the Belgian National Fund for Scientific Research F.R.S.-FNRS. Financial support from this organization is acknowledged.

Conflicts of Interest: The authors declare no conflict of interest.

References

1. Kramida, A.; Ralchenko, Y.; Reader, J.; NIST ASD Team. NIST Atomic Spectra Database, National Institute of Standards and Technology, Gaithersburg. 2018. Available online: http://physics.nist.gov/asd (accessed on 6 January 2020).
2. Wybourne, B.G. The fascination of the rare earths—Then, now and in the future. *J. Alloy. Compd.* **2004**, *380*, 96. [CrossRef]
3. Lawler, J.E.; Den Hartog, E.A.; Sneden, C. Spectroscopic Data for Neutral and Ionized Rare Earth Elements. *AIP Conf. Proc.* **2005**, *771*, 152.
4. Wahlgren, C.M. The lanthanide elements in stellar and laboratory spectra. *Phys. Scr.* **2002**, *T100*, 22. [CrossRef]
5. Mumpower, M.R.; McLaughlin, G.C.; Surman, R. The Rare Earth Peak: An Overlooked r-process Diagnostic. *Astrophys. J.* **2012**, *752*, 117. [CrossRef]
6. Biémont, E.; Quinet, P. Recent Advances in the Study of Lanthanide Atoms and Ions. *Phys. Scr.* **2003**, *105*, 38. [CrossRef]
7. Cowley, C.R.; Mathys, G. Line identifications and preliminary abundances from the red spectrum of HD 101065 (Przybylski's star). *Astron. Astrophys.* **1998**, *339*, 165.
8. Cowley, C.R.; Ryabchikova, T.; Kupka, F.; Bord, D.J.; Mathys, G.; Bidelman, W.P. Abundances in Przybylski's star. *Mon. Not. R. Astron. Soc.* **2000**, *317*, 299. [CrossRef]
9. Gopka, V.F.; Ul'yanov, O.M.; Andrievskii, S.M. A hypothesis for explaining the origin of Przybylski's star (HD 101065). *Kin. Phys. Celest. Bodies* **2008**, *24*, 36.
10. Cowley, C.R. Lanthanide Rare Earths in Stellar Spectra With Emphasis on Chemically Peculiar Stars. *Phys. Scr.* **1984**, *8*, 28. [CrossRef]
11. Kasen, D.; Metzger, B.; Barnes, J.; Quataert, E.; Ramirez-Ruiz, E. Origin of the heavy elements in binary neutron-star mergers from a gravitational-wave event. *Nature* **2017**, *551*, 80. [CrossRef]

12. Pian, E.; d'Avanzo, P.; Benetti, S.; Branchesi, M.; Brocato, E.; Campana, S.; Getman, F. Spectroscopic identification of r-process nucleosynthesis in a double neutron-star merger. *Nature* **2017**, *551*, 67. [CrossRef] [PubMed]
13. Tanvir, N.R.; Levan, A.J.; González-Fernández, C.; Korobkin, O.; Mandel, I.; Rosswog, S.; Kangas, T. The emergence of a lanthanide-rich kilonova following the merger of two neutron stars. *Astrophys. J. Lett.* **2017**, *848*, L27. [CrossRef]
14. Metzger, B.D. Kilonovae. *Liv. Rev. Relat.* **2017**, *20*, 3. [CrossRef] [PubMed]
15. Gaigalas, G.; Kato, D.; Rynkun, P.; Radziuté, L.; Tanaka, M. Extended Calculations of Energy Levels and Transition Rates of Nd ii-iv Ions for Application to Neutron Star Mergers. *Astrophys. J. Suppl. Ser.* **2019**, *240*, 29. [CrossRef]
16. Hemmilä, I. Luminescent lanthanide chelates—A way to more sensitive diagnostic methods. *J. Alloy. Compd.* **1995**, *225*, 480.
17. Hasewaga, Y.; Wada, Y.; Yanagida, S. Strategies for the design of luminescent lanthanide(III) complexes and their photonic applications. *J. Photochem. Photobiol. C* **2004**, *5*, 183. [CrossRef]
18. Døssing, A. Luminescence from Lanthanide(3+) Ions in Solution. *Eur. J. Inorg. Chem.* **2005**, *2005*, 1425. [CrossRef]
19. Werts, M.H.V. Making sense of lanthanide luminescence. *Sci. Prog.* **2005**, *88*, 101. [CrossRef]
20. Cowan, R.D. *The Theory of Atomic Structure and Spectra*; University of California Press: Berkeley, CA, USA, 1981.
21. Quinet, P.; Palmeri, P.; Biémont, E.; McCurdy, M.M.; Rieger, G.; Pinnington, E.H.; Wickliffe, M.E.; Lawler, J.E. Experimental and theoretical lifetimes, branching fractions and oscillator strengths in Lu II. *Mon. Not. R. Astron. Soc.* **1999**, *307*, 934. [CrossRef]
22. Quinet, P.; Palmeri, P.; Biémont, E.; Li, Z.S.; Zhang, Z.G.; Svanberg, S. Radiative lifetime measurements and transition probability calculations in lanthanide ions. *J. Alloy. Compd.* **2002**, *344*, 255. [CrossRef]
23. Biémont, E.; Palmeri, P.; Quinet, P. A new database of astrophysical interest. *Astrophys. Space Sci.* **1999**, *269*, 635. [CrossRef]
24. Fraga, S.; Karwowski, J.; Saxena, K.M.S. *Handbook of Atomic Data*; Elsevier: Amsterdam, The Netherlands, 1976.
25. Johnson, W.R.; Kolb, D.; Huang, K.N. Electric-dipole, quadrupole, and magnetic-dipole susceptibilities and shielding factors for closed-shell ions of the He, Ne, Ar, Ni (Cu+), Kr, Pb, and Xe isoelectronic sequences. *At. Data Nucl. Data Tables* **1983**, *28*, 333. [CrossRef]
26. Hameed, S.; Herzenberg, A.; James, M.G. Core polarization corrections to oscillator strengths in the alkali atoms. *J. Phys. B* **1968**, *1*, 822. [CrossRef]
27. Hameed, S. Core Polarization Corrections to Oscillator Strengths and Singlet-Triplet Splittings in Alkaline Earth Atoms. *J. Phys. B* **1972**, *5*, 746. [CrossRef]
28. Biémont, E.; Quinet, P.; Svanberg, S.; Xu, H.L. Experimental lifetime determination in neutral praseaodymium (Pr I) and neodymium (Nd I). *J. Phys. B* **2004**, *37*, 1381. [CrossRef]
29. Biémont, E.; Lefèbvre, P.H.; Quinet, P.; Svanberg, S.; Xu, H.L. Radiative lifetime measurements and oscillator strength determination for transitions in singly ionized praseaodymium (Pr II). *Eur. Phys. J. D* **2003**, *27*, 33. [CrossRef]
30. Svanberg, S. *Atomic and Molecular Spectroscopy. Basic Aspects and Practical Applications*; Springer: Berlin/Heidelberg, Germany, 2001.
31. Engström, L.; Lundberg, H.; Nilsson, H.; Hartman, H.; Bäckström, E. The FERRUM project: Experimental transition probabilities from highly excited even 5s levels in Cr II. *Astron. Astrophys.* **2014**, *570*, A34. [CrossRef]
32. Gamrath, S.; Palmeri, P.; Quinet, P. Radiative transition parameters in atomic lanthanum from pseudo-relativistic Hartree-Fock and fully relativistic Dirac-Fock calculations. *Atoms* **2019**, *7*, 38. [CrossRef]
33. Den Hartog, E.A.; Palmer, A.J.; Lawler, J.E. Radiative lifetimes and transition probabilities of neutral lanthanum. *J. Phys. B* **2015**, *48*, 155001. [CrossRef]
34. Biémont, E.; Garnir, H.P.; Litzén, U.; Nielsen, K.; Quinet, P.; Svanberg, S.; Wahlgren, G.M.; Zhang, Z.G. Radiative lifetime and oscillator strength determinations in Sm III. *Astron. Astrophys.* **2003**, *399*, 343. [CrossRef]

35. Tian, Y.; Wang, X.; Liu, C.; Dai, Z. Measurements of radiative lifetimes, branching fractions, transition probabilities, and oscillator strengths for Eu II and Eu III levels. *Mon. Not. R. Astr. Soc.* **2019**, *485*, 4485. [CrossRef]
36. Yu, Q.; Wang, X.; Li, Q.; Gong, Y.; Dai, Z. Experimental radiative lifetimes, branching fractions, and oscillator strengths of some levels in Tm III. *Mon. Not. R. Astr. Soc.* **2018**, *476*, 4861. [CrossRef]
37. Öberg, K.J.; Lundberg, H. Experimental transition probabilities and improved level energies in Yb III. *Eur. Phys. J. D* **2007**, *42*, 15. [CrossRef]
38. Jorissen, A. Atomic and molecular data for stellar physics: Former successes and future challenges. *Phys. Scr.* **2004**, *112*, 73. [CrossRef]
39. Ryabchikova, T.; Mashonkina, L. The role of atomic and molecular data in stellar atmosphere studies: Atmospheric structure and chemistry. *Phys. Scr.* **2014**, *89*, 114007. [CrossRef]
40. Monier, R. Atomic data needs for the modelling of stellar spectra. *arXiv* **2015**, arXiv:1509.09165.
41. VALD. Available online: https://www.astro.uu.se (accessed on 6 January 2020).
42. VAMDC. Consortium. Available online: http://www.vamdc.org (accessed on 6 January 2020).
43. Reyniers, M.; Van Winckel, H.; Biémont, E.; Quinet, P. Cerium: The lithium substitute in post-AGB stars. *Astron. Astrophys.* **2002**, *395*, L35. [CrossRef]
44. Reyniers, M.; Van Winckel, H. Detection of elements beyond the Ba-peak in VLT+UVES spectra of post-AGB stars. *Astron. Astrophys.* **2003**, *408*, L33. [CrossRef]
45. Shavrina, A.V.; Polosukhina, N.S.; Pavlenko, Y.V.; Yushchenko, A.V.; Quinet, P.; Hack, M.; North, P.; Gopka, V.F.; Zverko, J.; Zhiznovsky, J.; et al. The spectrum of the roAp star HD 101065 (Przybylski's star) in the Li I 6708 Å spectral region. *Astron. Astrophys.* **2003**, *409*, 707. [CrossRef]
46. Drake, N.A.; Nesvacil, N.; Hubrig, S.; Kochukhov, O.; de la Reza, R.; Polosukhina, N.S.; Gonzalez, J.F. Spectroscopic analysis of chemically peculiar stars: Abundance determination of lithium and some rare earth elements. *Proc. Int. Astron. Union* **2005**, *1*, 89–90. [CrossRef]
47. Shavrina, A.V.; Polosukhina, N.S.; Khan, S.; Pavlenko, Y.V.; Kudryavtsev, D.O.; Khalack, V.R.; Mikhailitskaya, N.G.; Lyubchik, Y.P.; Yushchenko, A.V.; Hatzes, A.; et al. Lithium and the ^{6}Li–^{7}Li isotope ratio in the atmospheres of some sharp-lined roAp stars. *Astron. Rep.* **2006**, *50*, 500. [CrossRef]
48. Sneden, C.; Lawler, J.E.; Cowan, J.J.; Ivans, I.I.; Den Hartog, E.A. New rare earth element abundance distributions for the Sun and five r-process-rich very metal-poor stars. *Astrophys. J. Suppl. Ser.* **2009**, *182*, 80. [CrossRef]
49. Cowley, C.R.; Hubrig, S.; Palmeri, P.; Quinet, P.; Biémont, E.; Wahlgren, G.M.; Schütz, O.; Gonzalez, J.F. HD 65949: Rosetta stone or red herring. *Mon. Not. R. Astron. Soc.* **2010**, *405*, 1271. [CrossRef]
50. Elkin, V.G.; Kurtz, D.W.; Nitschelm, C.; Unda-Sanzana, E. The discovery of a 21-kG magnetic field in the Ap star BD+0°4535. *Mon. Not. R. Astron. Soc.* **2010**, *401*, L44. [CrossRef]
51. Shulyak, D.; Ryabchikova, T.; Kildiyarova, R.; Kochukhov, O. Realistic model atmosphere and revised abundances of the coolest Ap star HD 101065. *Astron. Astrophys.* **2010**, *520*, A88. [CrossRef]
52. Elkin, V.G.; Kurtz, D.W.; Mathys, G. HD 97394: A magnetic Ap star with high cerium overabundance. *Mon. Not. R. Astron. Soc.* **2011**, *415*, 2233. [CrossRef]
53. Niemczura, E.; Hümmerich, S.; Castelli, F.; Paunzen, E.; Bernhard, K.; Hambsch, F.J.; Helminiak, K. HD 66051, an eclipsing binary hosting a highly peculiar, HgMn-related star. *Nat. Sci. Rep.* **2017**, *7*, 5906. [CrossRef]
54. Yushchenko, A.V.; Gopka, V.F.; Shavrina, A.V.; Yushchenko, V.A.; Vasileva, S.V.; Andrievsky, S.M.; Raikov, A.A.; Kim, S.; Rittipruk, P.; Jeong, Y.; et al. Peculiarities of the abundance of chemical elements in the atmosphere of PMMR23-red supergiant in the small magellanic cloud due to interstellar gas accretion. *Kin. Phys. Celest. Bodies* **2017**, *33*, 199. [CrossRef]
55. Hümmerich, S.; Niemczura, E.; Walczak, P.; Paunzen, E.; Bernhard, K.; Murphy, S.J.; Drobek, D. A spectroscopic and photometric investigation of the mercury-manganese star KIC 6128830. *Mon. Not. R. Astron. Soc.* **2018**, *464*, 2467. [CrossRef]
56. Paunzen, E.; Fedurco, M.; Helminiak, K.G.; Pintado, O.I.; Hambsch, F.J.; Hümmerich, S.; Niemczura, E.; Bernhard, K.; Konacki, M.; Hubrig, S.; et al. Orbital parameters and evolutionary status of the highly peculiar binary system HD 66051. *Astron. Astrophys.* **2018**, *615*, A36. [CrossRef]
57. Tanaka, M.; Hotokezaka, K. Radiative transfer simulations of neutron star merger ejecta. *Astrophys. J.* **2013**, *775*, 113. [CrossRef]

58. Tanaka, M.; Hotokezaka, K.; Kyutoku, K.; Wanajo, S.; Kiuchi, K.; Sekiguchi, Y.; Shibata, M. Radioactively powered emission from black hole-neutron star mergers. *Astrophys. J.* **2014**, *780*, 31. [CrossRef]
59. Biémont, E.; Quinet, P.; Svanberg, S.; Xu, H.L. Lifetime measurements and calculations in La I. *Eur. Phys. J. D* **2004**, *30*, 157. [CrossRef]
60. Biémont, E.; Li, Z.S.; Palmeri, P.; Quinet, P. Radiative lifetimes in La III and oscillator strengths in La III and Lu III. *J. Phys. B* **1999**, *32*, 3409. [CrossRef]
61. Biémont, E.; Clar, M.; Enzonga Yoca, S.; Fivet, V.; Quinet, P.; Träbert, E.; Garnir, H.P. Atomic structure calculations and beam-foil observations of La IV. *Can. J. Phys.* **2009**, *87*, 1275. [CrossRef]
62. Palmeri, P.; Quinet, P.; Wyart, J.F.; Biémont, E. Theoretical lifetimes and oscillator strengths in Ce II. Application to the chemical composition of the Sun. *Phys. Scr.* **2000**, *61*, 323. [CrossRef]
63. Zhang, Z.G.; Svanberg, S.; Jiang, Z.; Palmeri, P.; Quinet, P.; Biémont, E. Natural radiative lifetimes in Ce II. *Phys. Scr.* **2001**, *63*, 122. [CrossRef]
64. Biémont, E.; Quinet, P.; Ryabchikova, T. Core-polarization effects in doubly ionized cerium (Ce III) for transitions of astrophysical interest. *Mon. Not. R. Astron. Soc.* **2002**, *336*, 1155. [CrossRef]
65. Zhang, Z.G.; Svanberg, S.; Quinet, P.; Palmeri, P.; Biémont, E. Time-resolved laser spectroscopy of multiply ionized atoms: Natural radiative lifetimes in Ce IV. *Phys. Rev. Lett.* **2001**, *87*, 273001. [CrossRef]
66. Palmeri, P.; Quinet, P.; Frémat, Y.; Wyart, J.F.; Biémont, E. Theoretical oscillator strengths in Pr III and application to some CP stars. *Astrophys. J. Suppl. Ser.* **2000**, *129*, 367. [CrossRef]
67. Biémont, E.; Garnir, H.P.; Palmeri, P.; Quinet, P.; Li, Z.S.; Zhang, Z.G.; Svanberg, S. Core-polarization effects and radiative lifetime measurements in Pr III. *Phys. Rev. A* **2001**, *64*, 022503. [CrossRef]
68. Enzonga Yoca, S.; Quinet, P. Decay rates for radiative transitions in the Pr IV spectrum. *J. Phys. B* **2013**, *46*, 145003. [CrossRef]
69. Xu, H.L.; Svanberg, S.; Cowan, R.D.; Lefèbvre, P.H.; Quinet, P.; Biémont, E. Theoretical and experimental lifetime and oscillator strength determination in singly ionized neodymium (Nd II). *Mon. Not. R. Astron. Soc.* **2003**, *346*, 433. [CrossRef]
70. Zhang, Z.G.; Svanberg, S.; Palmeri, P.; Quinet, P.; Biémont, E. Measurement of lifetimes by laser-induced fluorescence and determination of transition probabilities of astrophysical interest in Nd III. *Astron. Astrophys.* **2002**, *385*, 724. [CrossRef]
71. Enzonga Yoca, S.; Quinet, P. Relativistic Hartree-Fock calculations of transition rates for allowed and forbidden lines in Nd IV. *J. Phys. B* **2014**, *47*, 035002. [CrossRef]
72. Fivet, V.; Quinet, P.; Biémont, E.; Jorissen, A.; Yushchenko, A.V.; Van Eck, S. Transition probabilities in singly ionized promethium and the identification of Pm II lines in Przybylski's star and HR 465. *Mon. Not. R. Astron. Soc.* **2007**, *380*, 771. [CrossRef]
73. Fivet, V.; Quinet, P.; Biémont, E.; Jorissen, A.; Yushchenko, A.V.; Van Eck, S. Erratum: Transition probabilities in singly ionized promethium and the identification of Pm II lines in Przybylski's star and HR 465. *Mon. Not. R. Astron. Soc.* **2007**, *382*, 944. [CrossRef]
74. Xu, H.L.; Svanberg, S.; Quinet, P.; Garnir, H.P.; Biémont, E. Time-resolved laser-induced fluorescence lifetime measurements and relativistic Hartree-Fock calculations of transition probabilities in Sm II. *J. Phys. B* **2003**, *36*, 4773. [CrossRef]
75. Quinet, P.; Biémont, E. Radiative lifetime, oscillator strength and Landé factor calculations in doubly ionized europium (Eu III). *Mon. Not. R. Astron. Soc.* **2003**, *340*, 463. [CrossRef]
76. Biémont, E.; Kohnen, G.; Quinet, P. Transition probabilities in Gd III. *Astron. Astrophys.* **2002**, *393*, 717. [CrossRef]
77. Biémont, E.; Garnir, H.P.; Quinet, P.; Svanberg, S.; Zhang, Z.G. Time-resolved laser-induced fluorescence lifetime measurements and theoretical transition probabilities in Tb III. *Phys. Rev. A* **2002**, *65*, 052502. [CrossRef]
78. Zhang, Z.G.; Svanberg, S.; Palmeri, P.; Quinet, P.; Biémont, E. Experimental and theoretical studies of Dy III: Radiative lifetimes and oscillator strengths of astrophysical interest. *Mon. Not. R. Astron. Soc.* **2002**, *334*, 1–10. [CrossRef]
79. Biémont, E.; Palmeri, P.; Quinet, P.; Paquin, G.; Zhang, Z.G.; Somesfalean, G.; Svanberg, S. Measurement of radiative lifetimes and determination of transition probabilities of astrophysical interest in Ho III. *Mon. Not. R. Astron. Soc.* **2001**, *328*, 1085. [CrossRef]

80. Zhang, Z.G.; Somesfalean, G.; Svanberg, S.; Palmeri, P.; Quinet, P.; Biémont, E. Radiative lifetime measurements and oscillator strengths of astrophysical interest in Ho III. *Astron. Astrophys.* **2002**, *384*, 364. [CrossRef]
81. Xu, H.L.; Jiang, Z.; Zhang, Z.G.; Dai, Z.; Svanberg, S.; Quinet, P.; Biémont, E. Radiative lifetime measurements in Er II by time-resolved laser spectroscopy. *J. Phys. B* **2003**, *36*, 1771. [CrossRef]
82. Biémont, E.; Garnir, H.P.; Bastin, T.; Palmeri, P.; Quinet, P.; Li, Z.S.; Zhang, Z.G.; Lokhnygin, V.; Svanberg, S. Radiative lifetime measurements and transition probabilities of astrophysical interest in Er III. *Mon. Not. R. Astron. Soc.* **2001**, *321*, 481. [CrossRef]
83. Quinet, P.; Palmeri, P.; Biémont, E. On the use of the Cowan's code for atomic structure calculations in singly ionized lanthanides. *J. Quant. Spectrosc. Rad. Transf.* **1999**, *62*, 625. [CrossRef]
84. Li, Z.S.; Zhang, Z.G.; Lokhnygin, V.; Svanberg, S.; Bastin, T.; Biémont, E.; Garnir, H.P.; Palmeri, P.; Quinet, P. Radiative lifetime measurements in Tm III with time-resolved laser spectroscopy and comparisons with HFR calculations. *J. Phys. B* **2001**, *34*, 1349. [CrossRef]
85. Enzonga Yoca, S.; Quinet, P. Radiative decay rates for electric dipole, magnetic dipole and electric quadrupole transitions in triply ionized thulium (Tm IV). *Atoms* **2017**, *5*, 28. [CrossRef]
86. Biémont, E.; Dutrieux, J.F.; Martin, I.; Quinet, P. Lifetime calculations in Yb II. *J. Phys. B* **1998**, *31*, 3321. [CrossRef]
87. Li, Z.S.; Svanberg, S.; Quinet, P.; Tordoir, X.; Biémont, E. Lifetime measurements in Yb II with time-resolved laser spectroscopy. *J. Phys. B* **1999**, *32*, 1731. [CrossRef]
88. Biémont, E.; Quinet, P.; Dai, Z.; Jiang, Z.; Zhang, Z.G.; Xu, H.L.; Svanberg, S. Lifetime measurements and calculations in singly ionized ytterbium. *J. Phys. B* **2002**, *35*, 4743. [CrossRef]
89. Biémont, E.; Garnir, H.P.; Li, Z.S.; Lokhnygin, V.; Palmeri, P.; Quinet, P.; Svanberg, S.; Wyart, J.F.; Zhang, Z.G. Experimental and theoretical energy levels, transition probabilities and radiative lifetimes in Yb III. *J. Phys. B* **2001**, *34*, 1869. [CrossRef]
90. Zhang, Z.G.; Li, Z.S.; Svanberg, S.; Palmeri, P.; Quinet, P.; Biémont, E. Experimental and theoretical lifetimes in Yb III. *Eur. Phys. J. D* **2001**, *15*, 301. [CrossRef]
91. Wyart, J.F.; Tchang-Brillet, W.U.L.; Spector, N.; Palmeri, P.; Quinet, P.; Biémont, E. Extended analysis of the spectrum of triply-ionized ytterbium (Yb IV) and transition probabilities. *Phys. Scr.* **2001**, *63*, 113. [CrossRef]
92. Fedchak, J.A.; Den Hartog, E.A.; Lawler, J.E.; Palmeri, P.; Quinet, P.; Biémont, E. Experimental and theoretical radiative lifetimes, branching fractions, and oscillator strengths for Lu I and experimental lifetimes for Lu II and Lu III. *Astrophys. J.* **2000**, *542*, 1109. [CrossRef]
93. Dai, Z.; Jiang, Z.; Xu, H.L.; Zhang, Z.G.; Svanberg, S.; Biémont, E.; Lefèbvre, P.H.; Quinet, P. Time-resolved laser-induced fluorescence measurements of Rydberg states in Lu I and comparison with theory. *J. Phys. B* **2003**, *36*, 479. [CrossRef]